

Hadronic B decays and charm at Belle II

Sagar Hazra, on behalf of the Belle II collaboration
*Tata Institute of Fundamental Research,
Mumbai 400 005, India*



We report the measurements of various hadronic B decays at the Belle II experiment using a 362 fb^{-1} sample of electron-positron collisions collected at the $\Upsilon(4S)$ resonance. All results agree with the previous determination, and some of them are already competitive with the world's best measurement. In addition, we present a newly developed algorithm for D meson flavor tagging (discriminating between D^0 and \bar{D}^0) at Belle II.

1 Introduction

Measurement of hadronic B decays play an important role in the flavor physics program to test the standard model (SM) and its extensions. Decays mediated by Cabibbo-suppressed $b \rightarrow u$ and $b \rightarrow d, s$ loop transitions constitute sensitive probes for non-SM contributions. We can exploit isospin symmetry in some hadronic decays to construct various sum rules. One such sum-rule combines the branching fractions and CP asymmetries of $B \rightarrow K\pi$ decays, providing a null test with precision better than 1% in the SM¹. Similarly, the CKM angle ϕ_2/α can be determined by measuring various $B \rightarrow \pi\pi$ decays related by isospin symmetry. Belle II has a unique capability of studying jointly, and within a consistent experimental environment, all relevant final states of isospin-related B decays to put a stringent bound on the sum-rule test as well as to improve our knowledge of angle ϕ_2 . The CKM angle ϕ_3/γ is the SM candle for CP violation and is very reliably predicted. A measurement of this angle has been performed in an analysis of the $B \rightarrow DK$ decays. Lastly, we report a novel charm flavor tagger that would be important for CP violation and mixing studies in the charm sector.

21 2 Determination of signal yield

22 A key challenge in reconstruction of decay modes considered here is the large contamination from
 23 $e^+e^- \rightarrow q\bar{q}$ ($q = u, d, s, c$) background coupled with a small signal branching fraction. We use
 24 a binary-decision-tree classifier that combines a number of variables, most related to the event
 25 shape topology, which provide discrimination between the $B\bar{B}$ and $q\bar{q}$ events. To determine the
 26 signal yield, we rely on two kinematic variables: the energy difference $\Delta E = E_B^* - \sqrt{s}/2$ between
 27 the energy of the reconstructed B candidate and half the collision energy, and the beam-energy-
 28 constrained mass $M_{bc} = \sqrt{s/(4c^4) - (p_B^*/c)^2}$, which is the invariant mass of the B meson, with
 29 its energy being replaced by half the collision energy; all quantities are calculated in the $\Upsilon(4S)$
 30 frame.

31 3 Isospin sum-rule

32 The isospin sum-rule relation for the $B \rightarrow K\pi$ system provides a stringent null test of the SM¹,

$$I_{K\pi} = \mathcal{A}_{K^+\pi^-} + \mathcal{A}_{K^0\pi^+} \frac{\mathcal{B}(K^0\pi^+) \tau_{B^0}}{\mathcal{B}(K^+\pi^-) \tau_{B^+}} - 2\mathcal{A}_{K^+\pi^0} \frac{\mathcal{B}(K^+\pi^0) \tau_{B^0}}{\mathcal{B}(K^+\pi^-) \tau_{B^+}} - 2\mathcal{A}_{K^0\pi^0} \frac{\mathcal{B}(K^0\pi^0)}{\mathcal{B}(K^+\pi^-)} = 0, \quad (1)$$

33 where \mathcal{B} , \mathcal{A} , and τ are the branching fractions, direct CP asymmetries, and lifetimes of B mesons,
 34 respectively. We measure the time-integrated asymmetry for the CP eigenstate $B^0 \rightarrow K^0\pi^0$ by
 35 inferring the B -meson flavor (B^0 or \bar{B}^0) from that of the other B meson produced on the $\Upsilon(4S)$
 36 decay, using a category-based flavor tagger².

37 Figures 1 and 2 show the ΔE distributions of all four $K\pi$ final states. From the fits we
 38 obtain the following branching fractions,

$$\begin{aligned} \mathcal{B}(B^0 \rightarrow K^+\pi^-) &= [20.7 \pm 0.4(\text{stat}) \pm 0.6(\text{syst})] \times 10^{-6}, \\ \mathcal{B}(B^+ \rightarrow K^+\pi^0) &= [14.2 \pm 0.4(\text{stat}) \pm 0.9(\text{syst})] \times 10^{-6}, \\ \mathcal{B}(B^+ \rightarrow K^0\pi^+) &= [24.4 \pm 0.7(\text{stat}) \pm 0.9(\text{syst})] \times 10^{-6}, \\ \mathcal{B}(B^0 \rightarrow K^0\pi^0) &= [10.2 \pm 0.6(\text{stat}) \pm 0.6(\text{syst})] \times 10^{-6} \end{aligned}$$

39 and CP asymmetries

$$\begin{aligned} \mathcal{A}_{CP}(B^0 \rightarrow K^+\pi^-) &= -0.07 \pm 0.02(\text{stat}) \pm 0.01(\text{syst}), \\ \mathcal{A}_{CP}(B^+ \rightarrow K^+\pi^0) &= 0.01 \pm 0.03(\text{stat}) \pm 0.01(\text{syst}), \\ \mathcal{A}_{CP}(B^+ \rightarrow K^0\pi^+) &= -0.01 \pm 0.08(\text{stat}) \pm 0.05(\text{syst}), \\ \mathcal{A}_{CP}(B^0 \rightarrow K^0\pi^0) &= -0.06 \pm 0.15(\text{stat}) \pm 0.05(\text{syst}). \end{aligned}$$

The dominant contribution to the systematic uncertainties comes from the π^0 and K_S^0 recon-

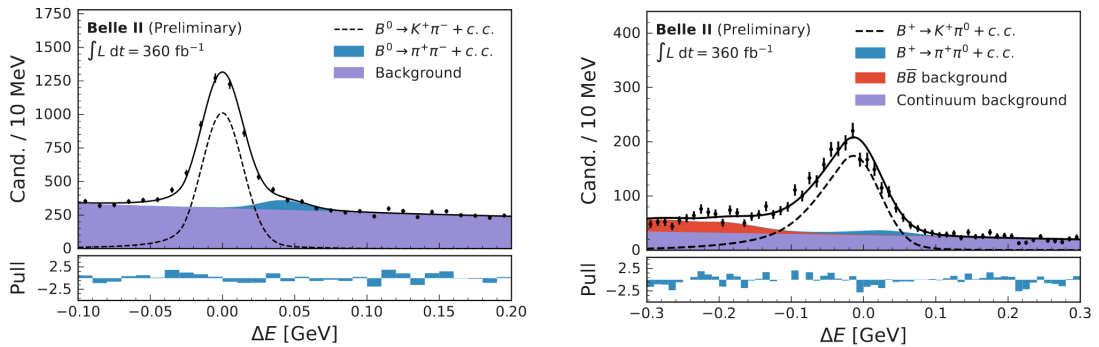


Figure 1 – Signal-enhanced ΔE distributions of $B^0 \rightarrow K^+\pi^-$ (left) and $B^+ \rightarrow K^+\pi^0$ (right).

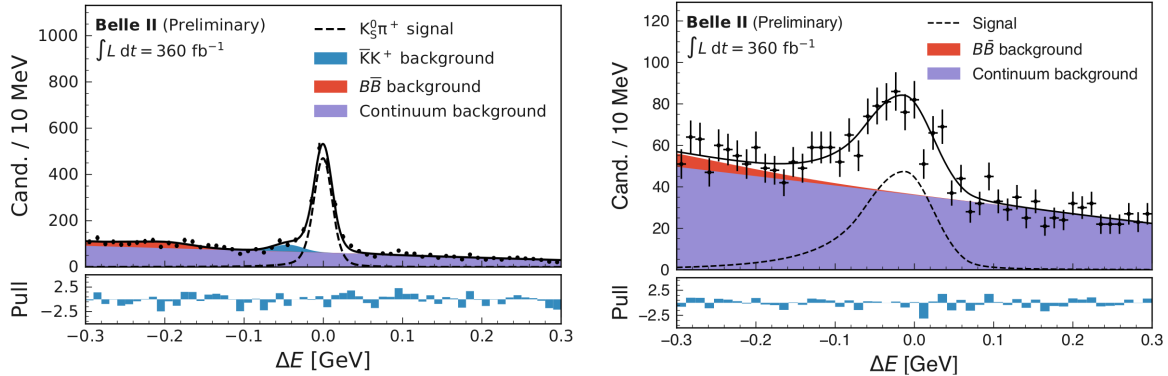


Figure 2 – Signal-enhanced ΔE distributions of $B^+ \rightarrow K^0\pi^+$ (left) and $B^0 \rightarrow K^0\pi^0$ (right).

40

41 reconstruction efficiencies for the decays having these final state particles. These are determined
 42 with the help of selected control samples and are expected to significantly decrease with the
 43 availability of larger sample sizes.

44

45 We also measure CP asymmetry in $B^0 \rightarrow K_S^0\pi^0$ decays using a time-dependent method.
 46 Additional motivation to perform this measurement is to determine the value of $\Delta\mathcal{S}_{CP} = \mathcal{S}_{CP} -$
 47 $\sin(2\phi_1)$ for the $b \rightarrow s$ loop transition, which is sensitive to potential NP contribution. The main
 48 challenge of this analysis is the absence of primary charged particles, which leads to poor decay
 49 time resolution. The analysis is validated with the $B^0 \rightarrow J/\psi K_S^0$ control sample, with the B
 50 decay time reconstructed using only the K_S^0 vertex. Figure 3 shows the reconstructed ΔE and
 Δt (difference in proper times between two B meson decays) distributions from which we obtain

$$\mathcal{A}_{CP} = 0.04_{-0.14}^{+0.15}(\text{stat}) \pm 0.05(\text{syst})$$

51 and

$$\mathcal{S}_{CP} = 0.75_{-0.23}^{+0.20}(\text{stat}) \pm 0.04(\text{syst}).$$

52

53 Precision of the measured mixing-induced asymmetry parameter \mathcal{S}_{CP} is already competitive
 54 with the world's best measurement although based on a small dataset.

55

56 We combine the time-dependent and time-integrated measurements to obtain the best sen-
 57 sitivity of $\mathcal{A}_{K_S^0\pi^0} = -0.01 \pm 0.12(\text{stat}) \pm 0.05(\text{syst})$. Putting all \mathcal{B} and \mathcal{A}_{CP} values of the $K\pi$
 58 system together, we obtain an overall Belle II isospin test:

$$I_{K\pi} = -0.03 \pm 0.13(\text{stat}) \pm 0.05(\text{syst}),$$

57

58 which is consistent with the SM prediction and comparable with world's best result (-0.13 ± 0.11)
 even with a smaller sample.

59 4 Towards the determination of ϕ_2

60

61 The combined analysis of branching fractions and CP violating asymmetries of the complete set
 62 of $B \rightarrow \pi\pi$ isospin partners enables a determination of ϕ_2 ³. We focus here on $B^+ \rightarrow \pi^+\pi^0$
 63 and $B^0 \rightarrow \pi^+\pi^-$ decays. Belle II has the unique capability to study all the $B \rightarrow \pi\pi$ decays to
 64 determine the CKM angle ϕ_2 . Figure 4 shows the ΔE distributions of $\pi^+\pi^0$ and $\pi^+\pi^-$ channels.

We obtain the following branching fractions,

$$\begin{aligned} \mathcal{B}(B^0 \rightarrow \pi^+\pi^-) &= [5.83 \pm 0.22(\text{stat}) \pm 0.17(\text{syst})] \times 10^{-6}, \\ \mathcal{B}(B^+ \rightarrow \pi^+\pi^0) &= [5.02 \pm 0.28(\text{stat}) \pm 0.32(\text{syst})] \times 10^{-6}, \end{aligned}$$

65

66 and CP asymmetry of $\mathcal{A}_{CP}(B^+ \rightarrow \pi^+\pi^0) = -0.08 \pm 0.05(\text{stat}) \pm 0.01(\text{syst})$. The dominant
 contribution in the systematic uncertainties comes from π^0 reconstruction and tracking efficiency.

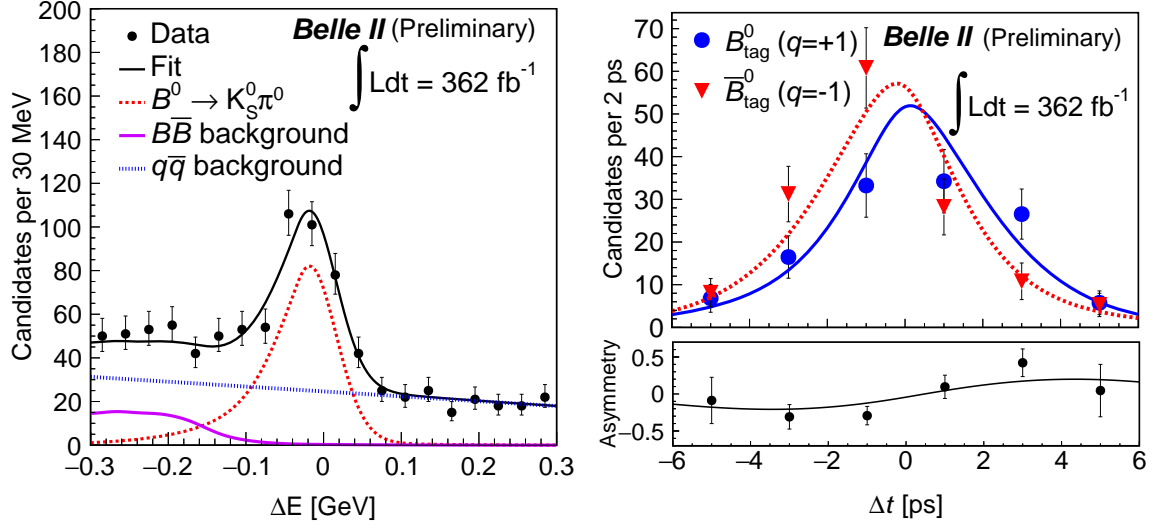


Figure 3 – Signal-enhanced ΔE distribution (left) and background subtracted B^0 and \bar{B}^0 -tag Δt distribution (right) for $B^0 \rightarrow K_S^0 \pi^0$ time-dependent CP asymmetry measurement.

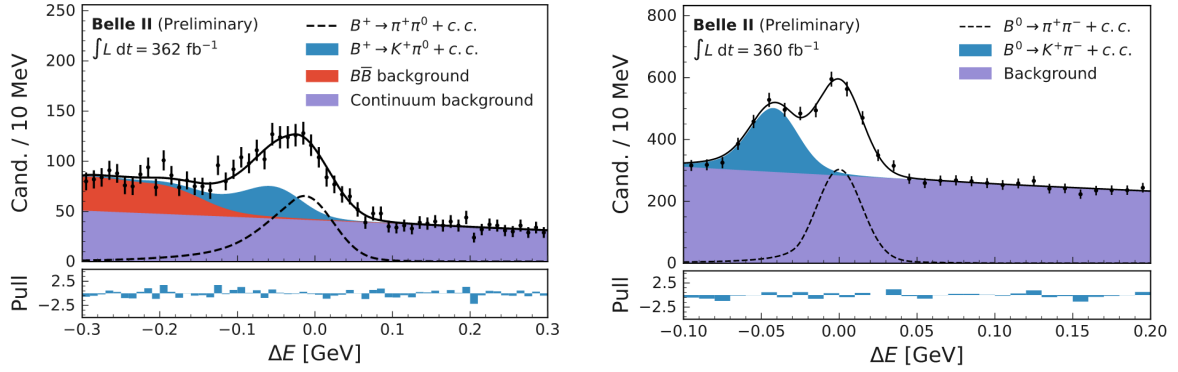


Figure 4 – Signal-enhanced ΔE distributions of $B^+ \rightarrow \pi^+ \pi^0$ (left) and $B^0 \rightarrow \pi^+ \pi^-$ (right).

67 5 Determination of ϕ_3/γ

68 The CKM angle ϕ_3/γ is a SM benchmark as it is the only angle accessed using tree level B
69 decays. The angle ϕ_3 is governed by interference between the favoured $b \rightarrow c\bar{u}s$ and suppressed
70 $b \rightarrow u\bar{c}s$ transitions in the $B \rightarrow DK$ decays:

$$\frac{\mathcal{A}_{\text{sup}}(B^- \rightarrow \bar{D}^0 K^-)}{\mathcal{A}_{\text{fav}}(B^- \rightarrow \bar{D}^0 K^-)} = r_B e^{i(\delta_B - \gamma)}, \quad (2)$$

71 where δ_B is the strong phase difference and r_B is the magnitude of the suppression. The angle ϕ_3
72 can be measured using different modes based on a different possible D final states. We present
73 the determination of ϕ_3 using GLW^{4,5} and GLS⁶ methods with Belle and Belle II datasets.

74 The GLW method uses the $D \rightarrow K^+ K^-$ (CP -even) and $D \rightarrow K_S^0 \pi^0$ (CP -odd) eigenstate to
75 determine ϕ_3 from $\mathcal{R}_{CP\pm} = 1 + r_B^2 \pm 2r_B \cos \delta_B \cos \phi_3$ and $\mathcal{A}_{CP\pm} = \pm 2r_B \sin \delta_B \sin \phi_3 / \mathcal{R}_{CP\pm}$.
76 This analysis used a combined Belle (711 fb^{-1}) and Belle II (189 fb^{-1}) data sample. We find the
77 following relative branching fractions,

$$\begin{aligned} \mathcal{R}_{CP+} &= (1.16 \pm 0.08(\text{stat}) \pm 0.04(\text{syst}))\%, \\ \mathcal{R}_{CP-} &= (1.15 \pm 0.07(\text{stat}) \pm 0.02(\text{syst}))\% \end{aligned}$$

78 and CP -violating rate asymmetries,

$$\begin{aligned}\mathcal{A}_{CP+} &= (+12.5 \pm 5.8(\text{stat}) \pm 1.4(\text{syst}))\%, \\ \mathcal{A}_{CP-} &= (-16.7 \pm 5.7(\text{stat}) \pm 0.6(\text{syst}))\%.\end{aligned}$$

79 While the results for CP -even eigenstate are not yet competitive with the world average, the
80 CP -odd eigenstate results achieve world's best measurement as it is a unique channel for the
81 Belle II.

82 The GLS method uses the Cabibbo-suppressed channels $B^\pm \rightarrow D(\rightarrow K_S^0 K^\pm \pi^\mp)h^\pm$ (same
83 sign) and $B^\mp \rightarrow D(\rightarrow K_S^0 K^\pm \pi^\mp)h^\mp$ (opposite sign) to determine 4 CP asymmetries and 3
84 branching ratios. This analysis used the combined Belle (711 fb^{-1}) and Belle II (362 fb^{-1}) data
85 sample. While the results are not competitive with world average, they still provide a constraint
86 on the measurement on ϕ_3 . This results will be used for the combination of ϕ_3 measurement
87 with Belle and Belle II data sample. We find the following ratio of branching fractions,

$$\begin{aligned}\mathcal{A}_{SS}^{DK} &= -0.089 \pm 0.091 \pm 0.011, \\ \mathcal{A}_{OS}^{DK} &= +0.109 \pm 0.133 \pm 0.013, \\ \mathcal{A}_{SS}^{D\pi} &= +0.018 \pm 0.026 \pm 0.009, \\ \mathcal{A}_{OS}^{D\pi} &= -0.028 \pm 0.031 \pm 0.009,\end{aligned}$$

88 and CP -violating rate asymmetries,

$$\begin{aligned}\mathcal{R}_{SS}^{DK/D\pi} &= 0.122 \pm 0.012 \pm 0.004, \\ \mathcal{R}_{OS}^{DK/D\pi} &= 0.093 \pm 0.013 \pm 0.003, \\ \mathcal{R}_{SS/OS}^{D\pi} &= 1.428 \pm 0.057 \pm 0.002.\end{aligned}$$

89 6 The charm flavor tagger

90 Identification of the D^0 flavor plays a crucial role in the CP -violation and mixing measurement
91 in the charm sector. Typically all the charm analysis uses the conventional D^* -tagging method
92 which has high purity but substantially reduces the data sample size. The main motivation for
93 developing a new algorithm is to also include D^0 mesons that do not emerge from a D^* decay.
94 The new charm flavor tagger uses boosted-decision-trees to recover additional flavor information
95 from the extra charged particles. Figure 5 shows a good agreement between the calibrated and
96 true flavor dilution. The novel charm flavor tagger has an effective tagging power,

$$\epsilon_{\text{tag}}^{\text{eff}} = (47.91 \pm 0.07(\text{stat}) \pm 0.51(\text{syst}))\%,$$

97 which is calculated in the $D^0 \rightarrow K^- \pi^+$ decays. Effective increase in the sample size is estimated
98 to evaluate the impact of charm flavor tagger in physics analysis. Figures 6 shows the effect of
99 charm flavor tagger on $D^* \rightarrow D^0[\rightarrow K^+ \pi^- \pi^0] \pi^+$ decays. We find for $D^0 \rightarrow K^- \pi^+$, doubling
100 the effective sample size compared to conventional D^* -tagged decays.

101 7 Conclusions

102 In summary, hadronic B decays and charm physics play an important role in sharpening flavor
103 picture. Belle II has unique access to channels that offer key tests of the SM. We have shown
104 five new results: CP violation in $B^0 \rightarrow K_S^0 \pi^0$ that probes isospin sum rule with world leading
105 precision, precise measurements of various two-body decays related to the extraction of angle
106 ϕ_2 , joining forces with Belle sample to offer most up-to-date information on ϕ_3 from GLW and
107 GLS analyses, and a novel neutral charm tagger that nearly doubles the tagged D meson sample
108 size.

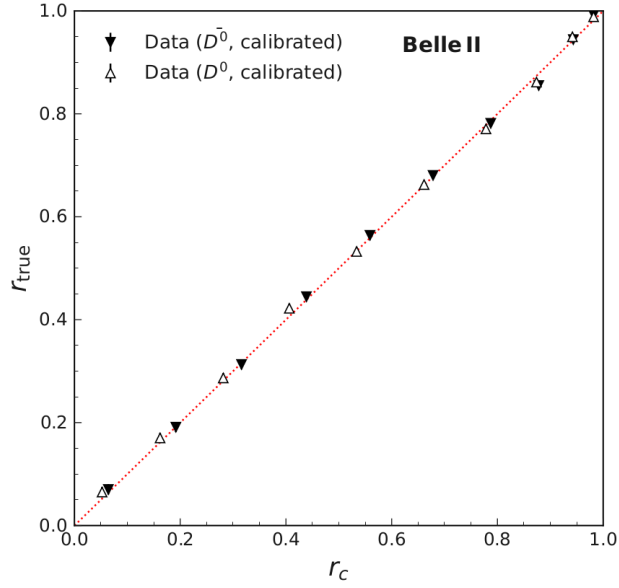


Figure 5 – True dilution as a function of calibrated dilution for $D^0 \rightarrow K^- \pi^+$ decays.

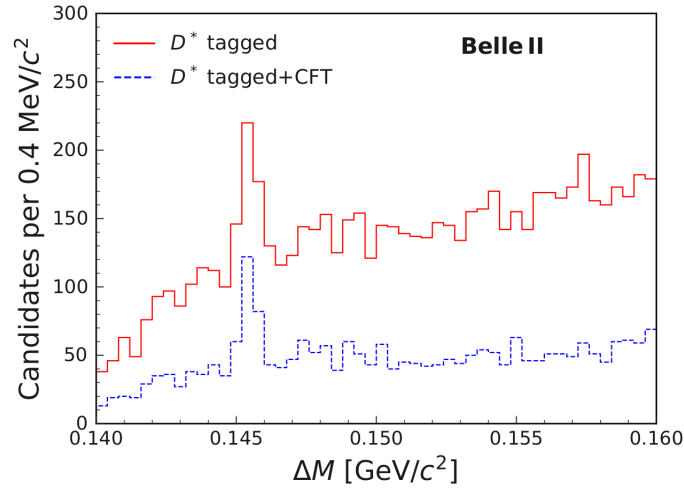


Figure 6 – Distribution of the difference between D^* and D^0 mass for the $D^* \rightarrow D^0[\rightarrow K^+ \pi^- \pi^0] \pi^+$ decays.

109 8 Acknowledgement

110 The author thanks to the Infosys Foundation for providing the leading edge travel grant.

111 References

- 112 1. M. Gronau, Phys. Lett. B **627**, 82 (2005).
 113 2. F. Abudinén *et al.* (Belle II Collaboration), Eur. Phys. J. C **82**, 283 (2022).
 114 3. M. Gronau and D. London, Phys. Rev. Lett. **65**, 3381 (1990).
 115 4. M. Gronau and D. London, Phys. Lett. B, **253(3)**, 483–488(1991).
 116 5. M. Gronau and D. Wyler, Phys. Lett. B, **265(1)**, 172–176 (1991).
 117 6. Z. Ligeti Y. Grossman and A. Soffer, Phys. Rev. D, **67**, 071301 (2003).